

Classification of Early Childhood Caries (ECC) Severity Using Spectroscopic Analysis and Artificial Intelligence

Siti Norbaieah Mohd Hashim^a, Ahmad Hussain Falaki^a, Rania Hussein Alashwal^a, Raja Kamarulzaman Raja Ibrahim^b, Tan Tian Swee^{c,d}, Maheza Irna Mohamad Salim^{a*}

^aDiagnostic Research Group, Health and Wellness Research Alliance, Universiti Teknologi Malaysia, 81310 UTM Johor Bahru, Johor, Malaysia; ^bFaculty of Sciences, Universiti Teknologi Malaysia, 81310 UTM Johor Bahru, Johor, Malaysia; ^cBioinspired Device and Tissue Engineering Research Group, Department of Biomedical Engineering and Health Sciences, Faculty of Electrical Engineering, Universiti Teknologi Malaysia, Johor Bahru, Johor, Malaysia; ^dIJN-UTM Cardiovascular Engineering Centre, Institute of Human Centered Engineering, Universiti Teknologi Malaysia, Johor Bahru, Johor, Malaysia

Abstract Early childhood caries (ECC) continues to pose a significant challenge for preschoolers worldwide, with a global prevalence of 46.2% in 2020. In the modern world of telehealth prominence, addressing ECC screening efficiently can be achieved through the integration of AI technology and saliva sample analysis. This framework allows parents and teachers to collect saliva samples from the children remotely to reduce the need for in-person healthcare visits. These samples will then be sent to healthcare facilities for analysis and attention will be given to screening results that indicate medium to high caries risk. In this study, a cohort of 104 kindergarten students have voluntarily provided saliva samples, along with additional parameters like pH, viscosity, quantity of saliva and hydration. The saliva was analyzed using the laser-induced breakdown spectroscopy (LIBS) and the results were used for artificial neural network (ANN) development to classify ECC severity. Two ANN models were developed with Model I used multivariate inputs consisting of pH, viscosity, hydration and spectroscopic saliva results whilst model II is developed based on spectroscopic saliva results only. Both ANN models are capable of effectively predicting ECC risk categories. The first model with multivariate inputs achieved performance accuracy of 91.8% whilst the second model, which relies solely on saliva spectroscopic data, exhibited performance accuracy of 92.7%. This study concluded that the use of telehealth and modern technologies such as LIBS and AI for ECC screening is helpful in ensuring a more accessible and efficient healthcare for young children by revolutionizing the healthcare approach.

***For correspondence:**

maheza@utm.my

Received: 06 Aug. 2024

Accepted: 20 Feb. 2025

©Copyright Mohd Hashim.

This article is distributed under the terms of the

Creative Commons Attribution License, which permits unrestricted use and redistribution provided that the original author and source are credited.

Introduction

Early Childhood Caries

Early childhood caries (ECC) is a dental condition that predominantly impacts children under the age of six. Recently, the WHO has reported that a concerning proportion of children experience decay and destruction of their teeth due to dental caries [1]. For instance, in 2020 alone, the global prevalence of dental caries in primary teeth stands at 46.2% while for permanent teeth is 53.8% [2]. Despite being largely preventable, ECC still stands as the most prevalent chronic condition affecting children worldwide [3, 5-7]. The WHO also reports a significant increase in ECC, particularly in economically disadvantaged

communities of low to mid-income countries [1] making ECC a significant global noncommunicable disease (NCD) with profound medical, social and economic implications [1,8]. Several studies reported higher ECC prevalence in developing countries or among disadvantaged children [3, 9-12]. Evidence also suggests that the actual prevalence depends on a country's ECC data availability, which, in turn, correlates with the number of dentists and physicians in the country and its economic development [13].

The term 'early childhood caries' is used to better encapsulate the multiple factors contributing to dental caries in young children, moving away from the earlier association of ECC solely with feeding methods [3,4]. ECC refers to tooth decay that includes cavities, missing teeth caused by decay, or teeth with fillings in primary teeth [4]. Concerning clinical presentation and diagnosis, ECC is a result of erosion of tooth enamel and dentin caused by acids produced by bacteria present in dental plaque, which builds up on the tooth surface. This erosion is a consequence of bacterial metabolism breaking down dietary sugars [1]. At an early stage, ECC manifests as dull white spots on the occlusal or gingival enamel surfaces of the teeth. This is followed by the first signs of decay which commonly appear on the four maxillary incisors as cavitated yellow or brown areas. Untreated lesions may progress further, creating black collars on the teeth surface and causing substantial hard tissue loss [3,5].

As caries lesions tend to progress more rapidly in primary dentition compared to permanent teeth, early detection of these lesions is crucial to effectively manage ECC and mitigate its associated complications [14]. Early detection is advantageous as it is not only likely to be painless for the child but also less costly [15]. Hence, caregivers of children under six years old play a vital role in this process together with healthcare professionals in ensuring a smooth early detection process [15]. Many countries have adopted the practice of incorporating oral health check-ups into preschool programs as a proactive measure to detect ECC at an early stage [14,16]. Dental teams are dispatched to preschools to conduct these check-ups, with the aim to facilitate ECC early diagnosis and promote oral health awareness among young children [17-18]. However, the implementation of this routine has been disrupted during the pandemic period due to movement restrictions and safety concerns.

The rise of telehealth and remote healthcare solutions has indeed provided a unique and timely opportunity to address health issues such as ECC more efficiently [27-30]. This shift towards remote healthcare has been further accelerated by the challenges posed by the COVID-19 pandemic. While the pandemic has highlighted the vulnerabilities of our healthcare systems, it has also propelled the development and adoption of innovative solutions to ensure uninterrupted healthcare delivery in the post-COVID era [31-32].

In this context, the emergence of an automated ECC detection system based on saliva analysis holds great promise. This framework enables parents and teachers to remotely collect saliva samples from children and students to minimize the need for physical visits to healthcare facilities. This not only reduces the risk of exposure to infectious diseases, such as COVID-19, but also addresses the practical challenges often associated with taking young children to healthcare appointments [27-30]. Additionally, the ability to collect saliva samples at home or in a school setting for ECC screening simplifies the process and makes it more convenient for both caregivers and children [28, 33-34]. Therefore, this research attempts to propose a new framework for early diagnosis of ECC by leveraging remote healthcare solutions and saliva sample analysis. Through this process, markers associated with an increased risk of ECC are assessed to stratify children into different risk categories.

Laser-Induced Breakdown Spectroscopy (LIBS) for ECC Analysis Using Saliva

Laser-Induced Breakdown Spectroscopy (LIBS), is a powerful spectroscopic technique utilizing high-energy laser light for chemical analysis, irrespective of the sample's state [35-36]. Previous studies reported that saliva contains various elements and microbial components that are relevant for assessing caries risk and progression [19-22]. This is because, dental decay alters teeth's chemical components and composition of saliva to reflect the decay level and provide clues to the status of oral health. For instance, healthy teeth have high calcium and phosphorus levels whilst copper and magnesium may accumulate in the saliva due to dentin demineralization caused by caries [37]. Additionally, salivary quantity and flow rate also play crucial roles in the development of ECC. Flow rate affects the dilution and removal of acids produced by bacteria. Flow rates below 0.3 mL/min (unstimulated) and 0.7 mL/min (stimulated) are indicative of potential risk [19]. Similarly, the normal pH range of saliva (6.75-7.25) prevents enamel demineralization occurring below pH 5.5. Saliva's high buffer capacity on the other hand, helps stabilize plaque pH and promoting the remineralization of enamel [19, 23-26].

In 2017, Matsuura *et al* proposed a method to enhance the sensitivity of ECC through LIBS analysis. The study demonstrates that early caries can be differentiated from healthy enamel by establishing a

suitable threshold for the detected ratios [38]. Zahroh *et al* later, utilized LIBS to investigate the relationship between cigarette consumption and calcium levels in saliva. Specifically, the study reported that light, moderate, and heavy smokers exhibited 30%, 37%, and 51% increases in calcium emission intensity, respectively, compared to non-smokers. These findings suggest a demineralization process associated with smoking, where calcium dissolves from tooth lattice into saliva [39].

Machine Learning for ECC Classifications

Machine learning has become an essential tool in dentistry, by benefitting the advancements in big data, computational power and sophisticated algorithms over the past two decades. It has found applications across various dental disciplines, including operative dentistry, periodontics, orthodontics, oral and maxillofacial surgery and prosthodontics [43]. In particular, machine learning has been used extensively for diagnostic tasks, offering valuable assistance to dental professionals in disease classification, risk assessment and treatment planning [40-43]. Specifically for Early Childhood Caries (ECC) classification, AI techniques have shown great promise in enhancing diagnostic accuracy by identifying risk factors and predicting caries development in children. For instance, Karhade *et al.* applied an automated machine learning algorithm (AutoML) to classify children based on their ECC status using a dataset of 6,404 children aged three to five years. This study has also examined various predictors of ECC, such as age and parent-reported oral health status as well as evaluated their impact on classification accuracy [41]. In another study, artificial neural networks (ANNs) were employed to detect salivary levels of cystatin S in ECC patients and caries-free (CF) children. The study found that a logistic regression model incorporating salivary cystatin S levels and birth weight showed promise for differentiating ECC from CF children [42]. While these studies demonstrate the potential of AI in ECC classification, they also highlight some key limitations, including limited generalizability across different populations and a lack of model interpretability, which becomes the barriers to clinical application.

While AI and spectroscopy have been applied to dental diagnostics, the use LIBS in ECC classification remains largely underexplored. This study seeks to fill this gap by integrating LIBS with ANN to improve diagnostic accuracy for ECC. LIBS, with its potential for non-invasive, real-time analysis of saliva mineral composition, offers a novel approach to enhance the classification of ECC.

Materials and Methods

Overview

This research was conducted in accordance with ethical approval from the Medical Research Ethics Committee (MREC), National Medical Research Register (NMRR), Ministry of Health, Malaysia, with approval number NMRR 18-2017-40905 IIR. A cohort of 104 kindergarten students aged 5 to 6 from Johor Bahru, Johor, Malaysia, participated in this study and voluntarily contributed their saliva samples for further analysis. Written informed consent was obtained from the parents prior to data collection. LIBS analysis was conducted on fresh saliva to provide insights into saliva mineral composition. The severity of dental caries in the subjects was evaluated by dentists at a government dental clinic in Johor Bahru, where mouth score values were assigned for each saliva sample. Overall, the LIBS analysis data, supplementary parameters and mouth score values collectively constitute the dataset for this study.

ECC Data Distribution Based on Severity

Following dentist evaluation through physical oral examination, out of the 104 subjects, 61 (58.6%) showed no signs of caries. Thirty-one (29.8%) exhibited mild cases, while six (5.8%) each displayed moderate and severe cases. The data distribution and sampling are outlined in Table 1 and Table 2 respectively.

Table 1. Data distribution based on dental assessment by dentist for mouth scoring

Severity category	Count	Percentage (%)
Sound	61	58.6
Mild	31	29.8
Moderate	6	5.8
Severe	6	5.8
Total	104	100

Table 2. Data Sampling

Category	Total	Training	Testing	Validation
Sound	61	41	10	10
Mild	31	21	5	5
Moderate	6	4	1	1
Severe	6	4	1	1
Total	104	70	17	10
Percentage	100	67.3	16.3	16.3

For the purpose of ANN development, the dataset was divided into training, testing and validation sets using a commonly adopted ratio to ensure model robustness and generalizability. The training set comprised nearly 70% of the data to allow the ANN to learn patterns effectively. The testing set accounted for nearly 15% of the data to enable performance evaluation on unseen data, while the validation set also constituted around 15% to fine-tune hyperparameters and prevent overfitting. This division aligns with best practices in machine learning applications in healthcare [53-54] to ensure a balance between model training, performance assessment and generalization ability.

Saliva Collection and Data Analysis Using LIBS

Saliva samples were collected in the morning by using the passive drool technique. Collection was timed at least 30 minutes before meals and 10 minutes after brushing or rinsing to minimize diurnal variability effects. Prior to collection, a parental agreement form was distributed to be filled up by parents along with the health status assessment questionnaire. Upon collection, the samples were refrigerated immediately at 4°C and processed within 2 hours to prevent bacterial growth. Saliva pH was analyzed using a digital meter after standardization with pH 10 solution. LIBS was employed for multi-elemental analysis. SpectraSuite and Spectragraph software were used for spectrum processing. The saliva sample underwent at least 4 measurements to confirm the presence of detected elements. Finally, the saliva spectroscopic data from LIBS analysis with other parameters namely hydration, viscosity, pH, buffering capacity, and the quantity of stimulated saliva were then used as input for the development of ANN model.

ANN Development

In this study, the ANN development phase was divided into training, testing and validation. The training phase stands as a critical stage to ensure that the model could effectively learn the intricate relationship between inputs and target. During training, a few ANN parameters were iterated to find the optimum values as shown in table 3 and once the optimal networks were established, they were saved and subjected to testing datasets to evaluate the performance accuracy of the model. Subsequently, the same model was applied to a distinct validation dataset to ensure it doesn't under or overfit the data and can reliably predict caries severity across new datasets.

Table 3. ANN parameters iterated during training stage

Parameter	Range	No. of variations
Training functions	TRAINGDM vs TRAINLM	2
Number of Neurons	6 - 20	9
Epochs	500 - 20000	6
Learning Rate	0.01 - 0.5	6
Momentum Constant	0 - 1	8

The backpropagation neural network (BPNN) algorithm was chosen due to its established reliability in medical and dental applications, particularly in classification tasks [44-48]. BPNN enables efficient weight

adjustments through iterative learning to improve model accuracy over multiple training cycles. During the initial optimization process for the number of neurons, two training functions namely TRAINGDM and TRAINLM, that are based on BPNN algorithms were tested. In this very first iteration stage, TRAINGDM yielded lower mean square error (MSE) and higher performance accuracy across the complete dataset, leading to its adoption for all subsequent optimization phases compared to TRAINLM functions.

Furthermore, different activation functions were experimented with for both the hidden and output layers of the ANN. However, the default function settings in MATLAB, where purelin is used in the output layer and log-sigmoid (logsig) in the hidden layer, outperformed other configurations and produced results which aligned with findings in existing literature [48].

During the training phase for both models, five training parameters underwent optimization as shown in Table 3. Following each cycle of parameter adjustments and iterations, the best network which exhibits the lowest MSE value was identified [48]. The corresponding optimal parameter values from each cycle were then utilized for the subsequent parameter optimization. The table below outlines the utilized value ranges during the ANN training for all the five ANN parameters.

This iterative process allowed for the fine-tuning of training parameters to enhance model performance. The training phase was conducted separately for each model, each employing distinct data inputs. The NNTOOL in Matlab is used to facilitate network training as shown in Figure 1.

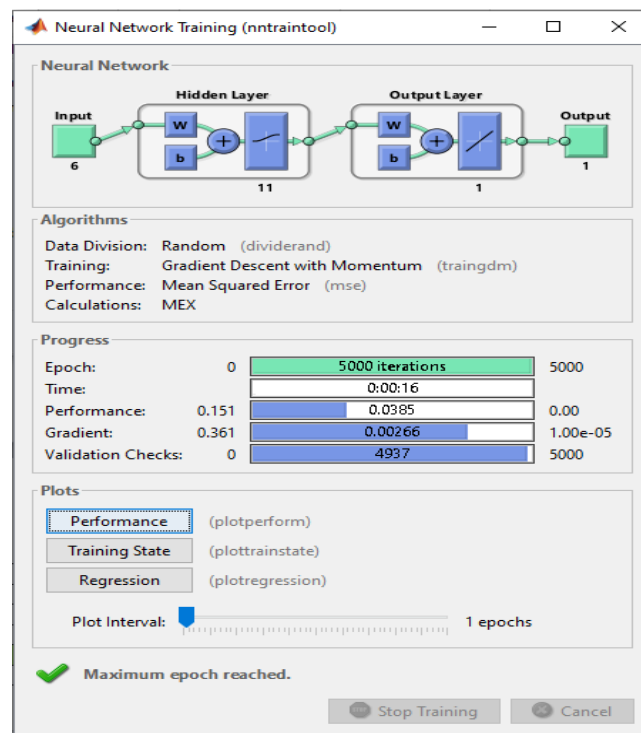


Figure 1. ANN model training facilitated by Matlab ANN Toolbox

For Model I, ten 1D input features were provided to the MATLAB trainer toolbox, while the output, representing the four severity classes earlier identified by professional dentists, served as the training target. The inputs are hydration, saliva quantity, viscosity, pH, and six LIBS spectral features corresponding to multiple isotopes of sodium, calcium, and copper. The training process was optimized by systematically adjusting the training parameters mentioned earlier. The network producing outputs closest to the actual targets was selected and saved as the model for the multiparameter model, designated as Model I.

For Model II training, the network input was restricted to the six 1D LIBS spectral features exclusively. Model II was trained following the same optimization regime and mirroring the process used in Model I training. The resulting optimal network was saved and designated as Model II.

Visualisation and Analysis

Testing and Validation

Evaluating the true capabilities of the two optimized network models requires the utilization of a fresh dataset that is distinctive from those employed during training. This process is used to gauge whether the networks can effectively predict the outcomes of new datasets. Model I underwent testing and validation using the Model I testing and validation datasets which comprises 10 inputs, while Model II was subjected to the same process using the Model II testing and validation datasets comprising 6 inputs. The target outputs remained consistent for both Model I and Model II which is the severity level decided by professional dentists.

Performance Assessment of the Model

Performance accuracy and Mean Squared Error (MSE) value were used to measure the performance of the developed models in each adjustment and iteration cycle. The top-performing network in each cycle is chosen based on its highest accuracy and lowest Mean Squared Error (MSE) performance.

Results and Discussion

LIBS Spectrum for Saliva

A total of 104 saliva samples were collected from volunteers among kindergarten students aged 5 to 6 from Johor Bahru, Johor, Malaysia. LIBS was employed for multi-elemental analysis of the salivary elements as shown in Figure 2. Small portion of the saliva sample was administered onto a stainless steel spoon and each saliva sample underwent at least 4 LIBS measurements to confirm the presence of any detected elements.

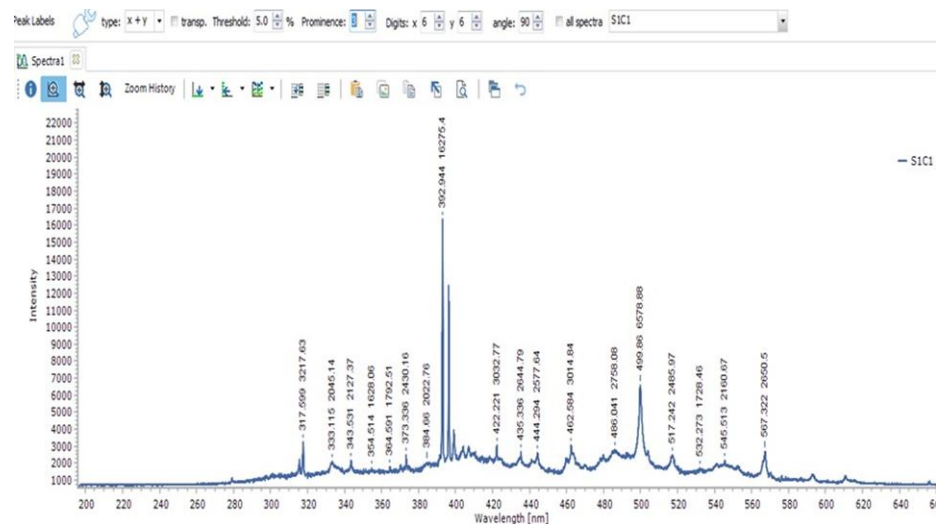


Figure 2. Sample of results from LIBS saliva analysis

Figure 2 displays the spectrum of the saliva sample against a stainless-steel background. From the results, it is shown that elements of Calcium (Ca), copper (Cu) and sodium (Na) were detected in the saliva sample. Calcium exhibited peaks at 399 nm and 391 nm, and this is consistent with findings by Choi *et al.* [11]. Additionally, copper (Cu) peaks at 324 nm whilst sodium showed three peaks, at 330 nm, 500 nm and 568 nm. The intensity of LIBS signals from these 6 different wavelength peaks make up the 6 LIBS elements inputted into the 2 models. For model I, additional oral parameters are added namely hydration, saliva quantity, viscosity, pH.

ANN Development Result

The training, testing and verification results of the two developed models were presented and compared in this particular section. The ECC dataset was partitioned into training, testing, and validation sets, approximately in a 70%:15%:15% ratio. Specifically, 70 samples were allocated to the training set, while 17 samples each were assigned to the testing and validation sets.

The initial training process was executed by comparing the performance of both the TRAINLM and TRAINGDM transfer functions as shown by the results in Figure 3 for Model I. The training results clearly show that the TRAINGDM function is capable of producing lower MSE values for all neuron count compared to the TRAINLM function for the same number of neurons. This suggests that TRAINGDM is more effective in minimizing prediction errors and improving model accuracy. This consistency has led to the decision of adopting TRAINGDM as the transfer functions of the developed ANN for further stages of the process.

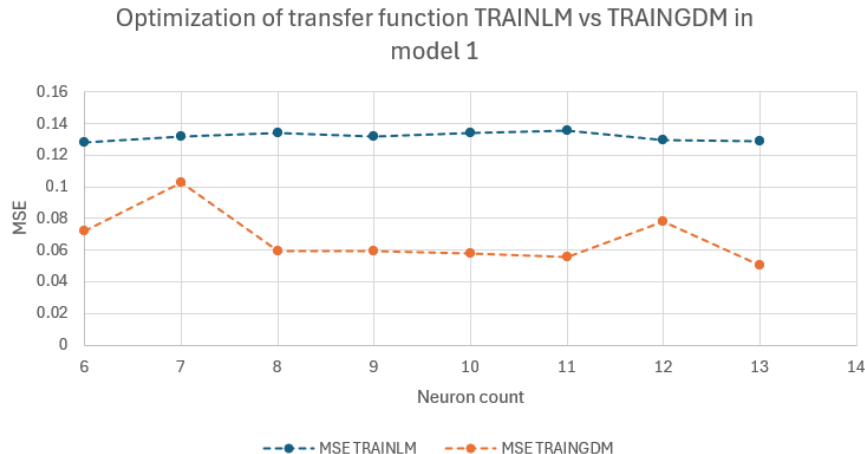


Figure 3. Optimization of Transfer functions TRAINLM vs TRAINGDM for Model I

The optimization of the neuron counts in the hidden layer was conducted right after the transfer function optimization. The results shown in Figure 4 demonstrated a clear trend of decreasing MSE values with higher neuron counts for Model I. As the number of neurons in the hidden layer increases from 6 to 20, the MSE values decrease. Specifically, the optimal MSE of 0.0443 is achieved with 14 neuron counts. On the other hand, there is no clear trend of MSE observed for Model II as the MSE values fluctuate with changes in the number of neurons. However, the lowest MSE was observed with 11 neuron counts at 0.0821.

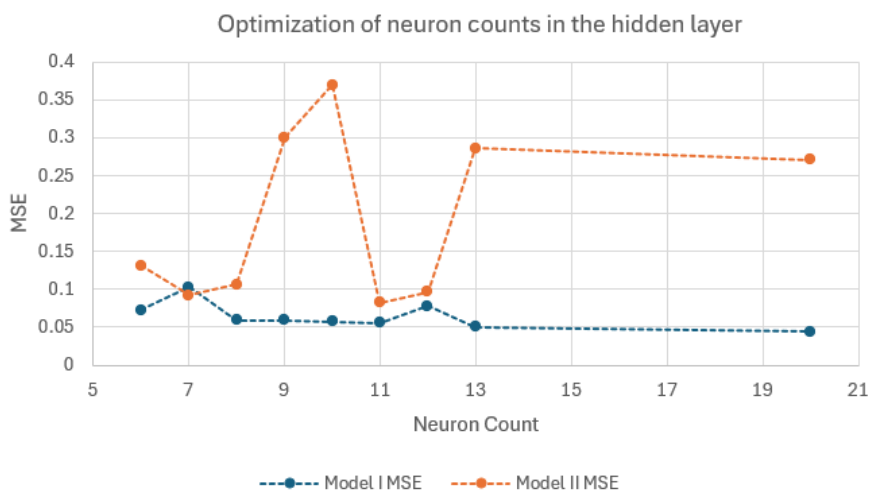


Figure 4. Optimization of neuron counts in the hidden layer

To optimize the iteration rate, the previously optimized number of neurons was kept constant while varying the epochs value over the selected range for both Model I and II. Figure 5 show that the best epoch for Model I is indicated by the lowest Mean Squared Error (MSE) value of 0.0448, occurring at

10000 epochs. Conversely, for Model II, the epoch with the lowest MSE value of 0.0722, observed at 5000 epochs. These results concluded that Model I has achieved its optimal performance after a longer training period, while Model II reaches its best performance relatively earlier in the training process. These findings suggest different learning dynamics and convergence rates between the two models.

In the process of learning rate optimization, the previously determined number of neurons and epochs for both models remained constant, while the learning rate values were systematically adjusted from 0.01 to 0.5, as depicted in the results in Figure 6. It is demonstrated that both models achieved its lowest MSE at a learning rate of 0.4. For Model I, MSE of 0.0285 was observed whilst for model II, the MSE is 0.0661. This finding suggests that a relatively moderate learning rate of 0.4 has contributed to a more efficient learning and improved the performance of both models.

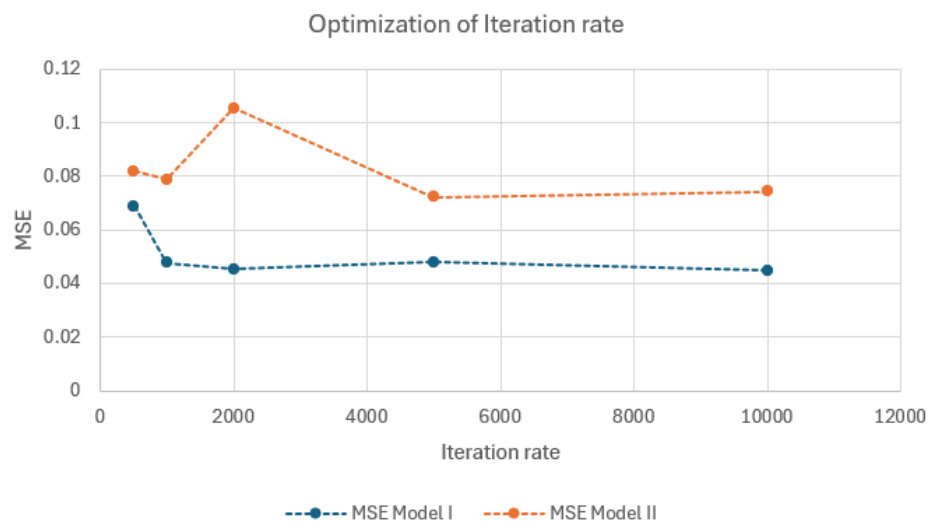


Figure 5. Relationship between Iteration rate and MSE in both models

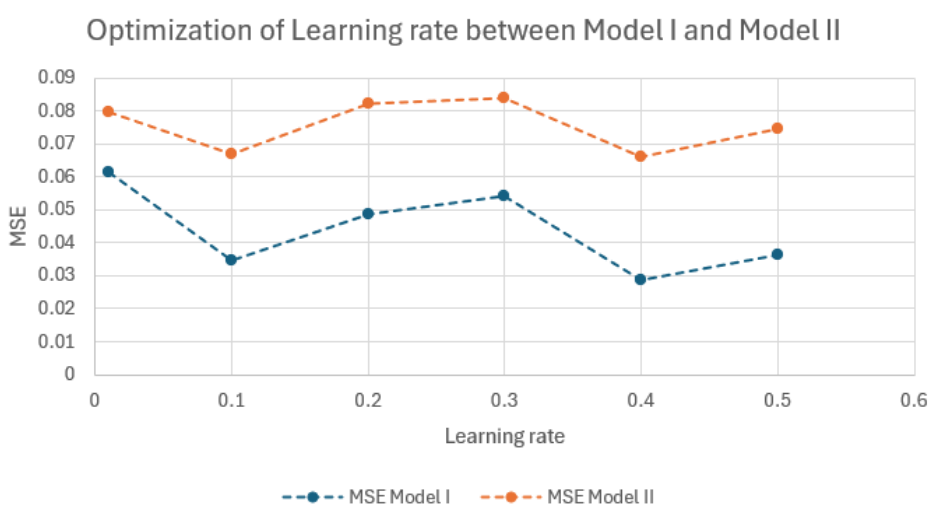


Figure 6. Relationship between learning rate and MSE

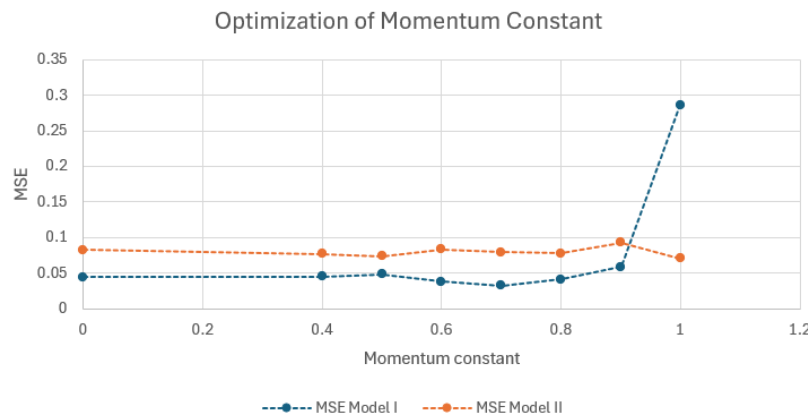


Figure 7. Relationship between MC and MSE for both models

In this study, the final training optimization was the momentum constant (MC). The momentum constant was fine-tuned across the range from 0 to 1 whilst the other ANN parameters determined earlier were kept constant. As shown in Figure 7, the results of the momentum constant optimization in this study reveals interesting insights into the performance of both Model I and Model II. For Model I, the MSE values generally decrease as the momentum constant increases up to the value of 0.7, indicating improved performance with higher momentum. However, beyond a momentum constant of 0.7, there is a slight increase in MSE, suggesting potential instability in the training process. On the other hand, for Model 2, the lowest MSE value is observed at a momentum constant of 1.0, indicating that higher momentum contributes to better performance in this case. Importantly, it's essential to balance the benefits of momentum with the risk of instability or overshooting, as observed with extremely high MSE at momentum values of 1.0 for Model I.

At the end of the optimization process, the overall architecture of the ANN is summarized in Table 4.

Table 4. Summary of optimal training parameters

ANN parameters	Model I	Model II
Number of neurons	14	11
Epochs	10000	5000
Learning rate	0.4	0.4
Momentum constant	0.7	1.0

ANN Testing and Validation

Table 5. Summary of Models Performances during training, testing and validation

Accuracy	Model I	Model II
Training (%)	96.7	92.9
Testing (%)	93.3	93.1
Validation (%)	91.8	92.7

Table 5 shows the results of the artificial neural network (ANN) training, testing and validation for both models. From the result, it is shown that in terms of training performance accuracy, Model I which is trained using 10 input parameters surpasses Model II which employs only LIBS data as input with a higher accuracy of 96.7% compared to Model II's accuracy of 92.9%.

This may indicate that Model I is more proficient at learning from the given training data and capable of capturing its underlying patterns. In the testing phase however, despite Model I's superior training accuracy during training, its accuracy slightly edges out Model II's accuracy, with Model I achieving 93.3% and Model II achieving 93.1%. This may suggest that while Model I excels in training, it may not be able to generalize as well to new data as Model II does during the testing phase. This trend may also be observed in previous studies on ANNs, where models exhibit varying generalization capabilities across different datasets and tasks [47-49]. Similar trends are observed in the validation phase, where Model II demonstrates a slightly higher accuracy of 92.7% compared to Model I's accuracy of 91.8%. This consistency across testing and validation phases [50] reinforces the facts that Model II exhibits slightly better generalization capabilities compared to Model I.

The overall high accuracy values obtained from both models show the reliability of the employed methodology and the substantial potential of the new framework as a new way of handling ECC in the post-pandemic era with the integration of AI and benefitting the concept of remote healthcare. This finding is consistent with previous studies where integrating multiple factors or data sources has been shown to enhance model performance [51]. This finding has also proven the feasibility of modifying the existing way of ECC management by introducing a screening process using saliva. This new framework which benefits the concept of telehealth [52], allows parents and teachers to collect saliva samples from their children and students for ECC screening remotely, to reduce the need for in-person healthcare visits. These samples will then be sent to healthcare facilities for further analysis and automated ECC severity screening interpretation. From this process, attention will be given to screening results indicating medium to high caries risk for further diagnosis and treatment.

Lastly, the dataset used in this study is subject to certain limitations. One notable issue is the presence of class imbalances, particularly regarding the distribution of moderate and severe ECC cases. A smaller number of samples in these categories may lead to biased model predictions, as the ANN could become more attuned to the more prevalent classes and could potentially reduce its sensitivity in detecting less common, yet clinically significant, severe cases. Class imbalance can result in the model to achieve high overall accuracy while underperforming in minority classes [53-54].

Conclusions

In conclusion, this research has demonstrated the efficacy of integrating ANN models in predicting the severity levels of ECC. Two distinct ANN models were successfully developed to classify ECC severity in this study. Model I utilized multivariate inputs consisting of pH, viscosity, hydration and spectroscopic saliva results and has achieved the accuracy of 91.8%, while Model II, which relied solely on saliva spectroscopic data exhibited a slightly higher accuracy of 92.7%. The superior performance of Model II highlights the significant influence of saliva spectroscopic data in determining ECC severity and demonstrated the potential of LIBS-based analysis as a standalone predictive tool.

Furthermore, this study also supports the feasibility of modifying the existing ECC management approach by integrating AI-driven screening using saliva samples. The proposed framework enables parents and teachers to remotely collect saliva samples from children for ECC screening, reducing the dependency on in-person healthcare visits and promoting more accessible and efficient early detection. The findings reinforce the potential of telehealth and modern technologies, such as LIBS and AI, in revolutionizing pediatric oral healthcare and ensuring timely intervention for young children.

Conflicts of Interest

The authors declare that there is no conflict of interest regarding the publication of this paper.

Acknowledgement

The authors would like to thank Universiti Teknologi Malaysia for the award of research grant Q.J130000.2651.15J83 on Detection of Early Dental Caries In Children Using Saliva Samples And Laser-Induced Breakdown Spectroscopy (LIBS).

References

- [1] World Health Organization. (2020). *Ending childhood dental caries: WHO implementation manual*. <https://www.who.int/publications/item/9789240000056>
- [2] Kazeminia, M., Abdi, A., Shohaimi, S., Jalali, R., Vaisi-Raygani, A., & Salari, N. (2020). Dental caries in primary and permanent teeth in children's worldwide, 1995 to 2019: A systematic review and meta-analysis. *Head & Face Medicine*, 16. <https://doi.org/10.1186/s13005-020-00233-7>
- [3] Alazmah, A. (2017). Early childhood caries: A review. *Journal of Contemporary Dental Practice*, 18(8), 732–737.
- [4] American Academy of Pediatric Dentistry. (2008). Definition of Early Childhood Caries (ECC). *American Academy of Pediatric Dentistry*, 4(age 3), 15.
- [5] Kamath, P. S., & G. S. (2017). Early Childhood Caries — A Review. *Journal of Dental and Orofacial Research*, 13(01).
- [6] Meyer, F., & Enax, J. (2018). Early Childhood Caries: Epidemiology, Aetiology, and Prevention. *International Journal of Dentistry*, 2018. <https://doi.org/10.1155/2018/1415873>
- [7] Pierce, A. et al. (2019). The Burden of Early Childhood Caries in Canadian Children and Associated Risk Factors. *Frontiers in Public Health*, 7.
- [8] Uribe, S. E. (2021). The global prevalence of early childhood caries: A systematic review with meta-analysis using the WHO diagnostic criteria. *International Journal of Paediatric Dentistry*, 31(6), 817–830. <https://doi.org/10.1111/ijpd.12759>
- [9] Baggio, S., Abarca, M., Bodenmann, P., Gehri, M., & Madrid, C. (2015). Early childhood caries in Switzerland: A marker of social inequalities. *BMC Oral Health*, 15(1), 1.
- [10] Anil, S., & Anand, P. S. (2017). Early childhood caries: Prevalence, risk factors, and prevention. *Frontiers in Pediatrics*, 5, 1. <https://doi.org/10.3389/fped.2017.00157>
- [11] Choi, D. et al. (2014). Laser-Induced Breakdown Spectroscopy (LIBS) Analysis of Calcium Ions Dissolved in Water Using Filter Paper Substrates: An Ideal Internal Standard for Precision Improvement. *Analytical Chemistry*, 86(2), 198–212. <https://doi.org/10.1021/ac402734v>
- [12] Goswami, P. (2020). Early Childhood Caries — A Review of Its Aetiology, Classification, Consequences, Prevention and Management. *Journal of Evolution of Medical and Dental Sciences*, 9(10), 798–803.
- [13] El Tantawi, M. et al. (2018). Prevalence and Data Availability of Early Childhood Caries in 193 United Nations Countries, 2007–2017. *American Journal of Public Health*, 108(8), 1066–1072. <https://doi.org/10.2105/AJPH.2018.304466>
- [14] Lokman, N., Husin, W., & Jamaludin, M. (2023). Multivariable Projections of Caries-Free Prevalence and the Associated Factors from 2019 to 2030 among Schoolchildren Aged 6, 12 and 16-Year-Old in Malaysia. *Children*, 10, 1125. <https://doi.org/10.3390/children1011125>
- [15] Zou, J. et al. (2022). Expert consensus on early childhood caries management. *International Journal of Oral Science*, 14(1), 35. <https://doi.org/10.1038/s41368-022-00155-2>
- [16] Chen, J. et al. (2021). Oral Health Policies to Tackle the Burden of Early Childhood Caries: A Review of 14 Countries/Regions. *Frontiers in Oral Health*, 2, 670154. <https://doi.org/10.3389/froh.2021.670154>
- [17] Yusof, Z. Y. M. et al. (2021). The effect of the SIMS Programme versus existing preschool oral healthcare programme on oral hygiene level of preschool children: Study protocol for a cluster randomised controlled trial. *Trials*, 22, 156. <https://doi.org/10.1186/s13063-021-05151-1>
- [18] Saikia, A., Aarthi, J., & Muthu, M. S. (2022). Sustainable development goals and ending ECC as a public health crisis. *Frontiers in Public Health*, 10, 931243. <https://doi.org/10.3389/fpubh.2022.931243>
- [19] Guo, L., & Shi, W. (2013). Salivary biomarkers for caries risk assessment. *Journal of California Dental Association*, 41(2), 107–109, 112–118.
- [20] Laputková, G., Schwartzová, V., Bánovčin, J., Alexovič, M., & Sabo, J. (2018). Salivary Protein Roles in Oral Health and as Predictors of Caries Risk. *Open Life Sciences*, 13, 174–200. <https://doi.org/10.1515/biol-2018-0022>
- [21] Pandey, P. et al. (2015). Estimation of salivary flow rate, pH, buffer capacity, calcium, total protein content and total antioxidant capacity in relation to dental caries severity, age and gender. *Contemporary Clinical Dentistry*, 6(Suppl 1), S65–S71. <https://doi.org/10.4103/0976-237X.152944>
- [22] Ravikumar, D. et al. (2023). Physical and chemical properties of saliva and its role in Early Childhood caries — A systematic review and meta-analysis. *Journal of Oral Biology and Craniofacial Research*, 13(5), 527–538. <https://doi.org/10.1016/j.jobcr.2023.04.003>
- [23] Farooq, I., & Bugshan, A. (2020). The role of salivary contents and modern technologies in the remineralization of dental enamel: A narrative review. *F1000Research*, 9, 171. <https://doi.org/10.12688/f1000research.22156.1>
- [24] Alkarad, L., Alkhouri, M., & Dashash, M. (2023). Remineralization of teeth with casein phosphopeptide-amorphous calcium phosphate: Analysis of salivary pH and the rate of salivary flow. *BDJ Open*, 9(1), 16. <https://doi.org/10.1038/s41405-023-00086-w>
- [25] Chen, X. et al. (2020). Microbial Etiology and Prevention of Dental Caries: Exploiting Natural Products to Inhibit Cariogenic Biofilms. *Pathogens*, 9(7), 569. <https://doi.org/10.3390/pathogens9070569>
- [26] Manchanda, S. et al. (2021). Is Mutans Streptococci count a risk predictor of Early Childhood Caries? A systematic review and meta-analysis. *BMC Oral Health*, 23(1), 648. <https://doi.org/10.1186/s12903-021-01928-2>
- [27] Syafriandi, S. et al. (2022). Feasibility of Using Saliva Samples and Laser-Induced Breakdown Spectroscopy for Dental Screening During Pandemic. In *6th Kuala Lumpur International Conference on Biomedical Engineering 2021*. Springer.
- [28] Azimi, S., Estai, M., Patel, J., & Silva, D. (2023). The feasibility of a digital health approach to facilitate remote dental screening among preschool children during COVID-19 and social restrictions. *International Journal of*

[29] *Paediatric Dentistry*, 33(3), 234–245. <https://doi.org/10.1111/13069>
Cianetti, S., Pagano, S., Nardone, M., & Lombardo, G. (2020). Model for Taking Care of Patients with Early Childhood Caries during the SARS-CoV-2 Pandemic. *International Journal of Environmental Research and Public Health*, 17(11), 3751. <https://doi.org/10.3390/ijerph17113751>

[30] Attia, D., ElKashlan, M. K., & Saleh, S. M. (2024). Early childhood caries risk indicators among preschool children in rural Egypt: A case control study. *BMC Oral Health*, 24, 10. <https://doi.org/10.1186/s12903-024-03334-6>

[31] Lee, S. M., & Lee, D. (2021). Opportunities and challenges for contactless healthcare services in the post-COVID-19 era. *Technological Forecasting and Social Change*, 167, 120712. <https://doi.org/10.1016/j.techfore.2021.120712>

[32] Sharma, A., Pruthi, M., & Sageena, G. (2022). Adoption of telehealth technologies: An approach to improving the healthcare system. *Translational Medicine Communications*, 7, 20. <https://doi.org/10.1186/s41231-022-00121-4>

[33] Haleem, A., Javaid, M., Singh, R. P., & Suman, R. (2021). Telemedicine for healthcare: Capabilities, features, barriers, and applications. *Sensors and Interventions*, 2, 100117. <https://doi.org/10.1016/j.snia.2021.100117>

[34] Amjad, A., Kordel, P., & Fernandes, G. (2023). A review on innovation in healthcare sector (telehealth) through artificial intelligence. *Sustainability*, 15, 6655. <https://doi.org/10.3390/su15086655>

[35] Anabitarte, F., Cobo, A., & López-Higuera, J. M. (2012). Laser-induced breakdown spectroscopy: Fundamentals, applications, and challenges. *ISRN Spectroscopy*, 2012. <https://doi.org/10.5402/2012/285240>

[36] Shah, S. et al. (2019). Laser induced breakdown spectroscopy methods and applications: A comprehensive review. *Radiation Physics and Chemistry*, 170. <https://doi.org/10.1016/j.radphyschem.2019.108665>

[37] Klimuszko, E. et al. (2018). Evaluation of calcium and magnesium contents in tooth enamel without any pathological changes: In vitro preliminary study. *Odontology*, 106. <https://doi.org/10.1007/s10266-018-0371-1>

[38] Matsuura, Y. (2017). Detection of early caries by laser-induced breakdown spectroscopy. In K. Sasaki, O. Suzuki, & N. Takahashi (Eds.), *Interface Oral Health Science 2016*. Springer, Singapore.

[39] Az Zahroh, A. M. T., & Nasution, H. S. (2018). The analysis of calcium contained in saliva due to smoking habits: Using laser-induced breakdown spectroscopy (LIBS). In *Proceedings of the Third International Seminar on Photonics, Optics, and Its Applications (ISPhOA 2018)* (Vol. 1104401).

[40] Ding, H. et al. (2023). Artificial intelligence in dentistry—A review. *Frontiers in Dental Medicine*, 4, 1085251. <https://doi.org/10.3389/fdmed.2023.1085251>

[41] Karhade, D. S. et al. (2021). An automated machine learning classifier for early childhood caries. *Pediatric Dentistry*, 43(3), 191–197.

[42] Koopaei, M. et al. (2021). Salivary cystatin S levels in children with early childhood caries in comparison with caries-free children: Statistical analysis and machine learning. *BMC Oral Health*, 21, 650. <https://doi.org/10.1186/s12903-021-01946-0>

[43] Vishwanathaiah, S. et al. (2023). Artificial intelligence its uses and application in pediatric dentistry: A review. *Biomedicines*, 11(3), 788. <https://doi.org/10.3390/biomedicines11030788>

[44] Xiao, Y. (2022). Application of neural network algorithm in medical artificial intelligence product development. *Computational and Mathematical Methods in Medicine*, 2022, 5413202. <https://doi.org/10.1155/2022/5413202>

[45] Yan, M. M. et al. (2022). Application of back propagation neural network model optimized by particle swarm algorithm. *The Journal of Clinical Hypertension*, 24(12), 1606–1617. <https://doi.org/10.1111/jch.14610>

[46] Ruan, F. et al. (2021). Back propagation neural network model for medical expenses in patients with breast cancer. *Mathematical Biosciences and Engineering*, 18(4), 3690–3698. <https://doi.org/10.3934/mbe.2021185>

[47] Arya, V. R., & Chandrasenan, A. (2014). Back propagation neural network-based detection and classification of brain tumors using Matlab. In *International Journal of Engineering Research & Technology (IJERT) NCETET – 2014* (Vol. 2, No. 08).

[48] Manaf, N. A. et al. (2016). Feasibility of A-mode ultrasound attenuation as a monitoring method of local hyperthermia treatment. *Medical & Biological Engineering & Computing*, 54, 967–981. <https://doi.org/10.1007/s11517-016-1452-3>

[49] Hamim, S. A., Tamim, M. U. I., Mridha, M. F., Safran, M., & Che, D. (2024). SmartSkin-XAI: An interpretable deep learning approach for enhanced skin cancer diagnosis in smart healthcare. *Diagnostics (Basel)*, 15(1), 64. <https://doi.org/10.3390/diagnostics15010064>

[50] Khan, A. Q., Awan, H. A., Rasul, M., Siddiqi, Z. A., & Pimanmas, A. (2023). Optimized artificial neural network model for accurate prediction of compressive strength of normal and high strength concrete. *Cleaner Materials*, 10, 100211. <https://doi.org/10.1016/j.clema.2023.100211>

[51] Liu, D., Qiao, Y., Wang, S., Fan, S., Liu, D., Shi, C., & Shi, J. (2024). A reliability estimation method based on combination of failure mechanism and ANN supported Wiener processes. *Helijon*, 10(4), e26230. <https://doi.org/10.1016/j.helijon.2024.e26230>

[52] Azimi, S., Estai, M., Patel, J., & Silva, D. (2023). The feasibility of a digital health approach to facilitate remote dental screening among preschool children during COVID-19 and social restrictions. *International Journal of Paediatric Dentistry*, 33(3), 234–245. <https://doi.org/10.1111/13069>

[53] Sivakumar, M., Parthasarathy, S., & Padmapriya, T. (2024). Trade-off between training and testing ratio in machine learning for medical image processing. *PeerJ Computer Science*, 10, e2245. <https://doi.org/10.7717/peerj-cs.2245>

[54] Ghasemzadeh, H., Hillman, R. E., & Mehta, D. D. (2024). Toward generalizable machine learning models in speech, language, and hearing sciences: Estimating sample size and reducing overfitting. *Journal of Speech, Language, and Hearing Research*, 67(3), 753–781. https://doi.org/10.1044/2023_JSLHR-23-00273